Solar System Wave Function and its Achievements

Abolfazl Soltani *

Department of Physics, University of Birjand, Birjand, Iran

***Email**: soltani.a.phyics@gmail.com*

Abstract

Pluto, Ceres and all planets of solar system except Neptune, with a high approximation, follow a law called Titius-Bode law (TBL) or Bode law, which can by no means be considered as a stochastic event. This law shows that the distance of the planets from the sun in Solar system is regulated. Here, we prove that the existence of a standing and cosine wave packet in solar system, with the wavelength $\lambda = 0.6\ AU$ (AU represents the distance of earth from the sun) and the phase constant $\emptyset_0 = \frac{\pi}{6}$, is the reason for TBL. Moreover, we prove that this huge wave packet belongs to the sun. We will prove that without solar system wave function, it is not possible to reach to the TBL from the protoplanetary disk of solar system. In the following of the article, based on the solar system wave function, we will enter into the atomic field and arrive to a new atomic model that helps us to describe many phenomena such as the normal Zeeman effect.

Keywords: Solar system, Titius-Bode law, Quantum mechanics, Atomic model, Schrodinger equation, Thought experiment, Normal Zeeman effect

1. Introduction

The planets of solar system move around the sun in elliptical orbits such that the sun is in one of the focal points of these ellipses. These ellipses are very close to the circle, and in fact the orbits of the planets of solar system are concentric circles. Pluto, Ceres and all planets of Solar system except Neptune, with a high approximation follow a law known as Bode law or Titius-Bode law (TBL). According to this law, the distance of each planet from the sun is equal to $a = 0.4\ AU + 0.3\ AU \times 2^n$, where $0.4\ AU$ is the distance of Mercury from the sun (or more precisely the length of the semi-major axis of Mercury's orbit) and $n = 0,1,2,3, \ldots$ [1]. Table. 1 shows the high accuracy of the Bode law. If this law was only true for three or four planets, then we could call it a coincidence, but when it is true for seven planets, plus Ceres and Pluto, there is definitely a reason for it. It was historically based on this law that Ceres was discovered in 1801 [1]. In this article, we will find the reason for the existence of the TBL. In fact, we will prove that the presence of a cosine and standing wave packet in solar system is the reason for existence of TBL; and moreover, we will prove that this wave packet belongs to the sun. In this article we prove that the Schrodinger equation is valid at the astronomical scale and is not limited to subatomic particles. TBL does not predict the distance of Neptune from the sun but, this article is able to give us the distance of Neptune. In this paper and in the section "Elliptical orbits and Isotropic Asteroid Belt", we prove that each model for explain the formation of solar system without considering the solar system wave function is incomplete and wrong. We will prove that without solar system wave packet, it is not possible to reach to the TBL from the protoplanetary disk.

Next, using the model of solar system standing wave, we enter into the fundamental topics of quantum mechanics and arrive at an atomic model that has both the Schrodinger wave function and the Bohr atomic model inside. Our atomic model explains why the Bohr atomic orbits are quantized (or In other words why the orbital angular momentum is quantized: $L = n\hbar$). Niels Bohr, neither in her famous article [2] nor in the years that followed, could not explain the reason for this event. The new atomic model predicts the existence of secondary lines in the hydrogen spectrum[1]. These are lines that neither the Bohr atomic model nor any other model has been able to explain [3][4][5][6]. Moreover, based on our new atomic model, we explain the reason of the normal Zeeman effect, etc.

Planet	T–B rule distance (AU)	Semi-major axis (AU)	Deviation from prediction
Mercury	0.4	0.39	−2.5%
Venus	0.7	0.72	+2.8%
Earth	1.0	1.00	0.00%
Mars	1.6	1.52	−4.77%
Ceres	2.8	2.77	−1.16%
Jupiter	5.2	5.20	+0.00%
Saturn	10.0	9.58	−4.45%
Uranus	19.6	19.20	−1.95%
Pluto	38.8	39.48	+1.05%

Table. 1. Planets distances from the sun and the prediction of Bode law. TBL cannot predict the distance of Neptune from the sun.

2. Wave Function and Bode Law

Consider a standing and cosine wave function with a wavelength $\lambda = 0.6\ AU$ in solar system; if we assume that the first node of this wave is at a distance of $0.1\ AU$ from the sun the next nodes are at the distances of $0.4\ AU$, $0.7\ AU$, $1\ AU$, $1.3\ AU$, $1.6\ AU$, ... $2.8\ AU$, … from the sun. Each node is $0.3\ AU$ ahead of the previous node. If we consider the planets of solar system in the position of the nodes of this wave, in such a case, there is no planet on the first node ($0.1\ AU$) and Mercury is on the second node, Venus is on the third node, earth is on the fourth node, Mars is on the sixth node, and the position of fifth node ($1.3\ AU$) is empty. The seventh, eighth, and ninth nodes are empty, and Ceres is on the tenth node. Jupiter is placed on the eighteenth node and Saturn is on the thirty-third node, and Uranus, Neptune, and Pluto are on the nodes farther from the sun. As you can see, a wave function, with the wavelength $\lambda = 0.6\ AU$, easily predicts the position of the planets and it seems that a huge and standing wave plays a role in determining the position of the planets in solar system. Therefore, we can consider the reason for the TBL to be the existence of a large cosine wave in solar system that oscillates along the axis perpendicular to the plane of solar

[1] Two series of lines appear in the spectrum of the hydrogen lamps. One series are the Ballmer, Lyman, Paschen, ... series. And the other lines called the secondary spectrum, which their number is very numerous and does not follow Rydberg equation: $\frac{1}{\lambda} = R(\frac{1}{n_{low}^2} - \frac{1}{n_{up}^2})$. Of course, this secondary spectrum is now known as the molecular spectrum, which this issue is based on Merton's article [3]. In this article, we show that this is wrong and only a part of the secondary spectrum lines is relevant to the hydrogen molecule.

system. We call this wave "Solar system wave function". In this article, we will obtain the equation of this wave function. But what does this wave belong to? We answer this question in this article. The presence of a huge cosine wave in solar system seems strange at first sight, but quantum mechanics eradicates our surprise. Based on quantum mechanics, a wave packet can be attributed to each object which called the "associated wave" of that object, and this associated wave is the solution of the Schrodinger equation. In this article, we prove that the above standing and cosine wave function (Solar system wave function) is in the form of a solution of the Schrodinger equation and therefore, based on quantum mechanics, this wave must belong to an object in Solar system; we demonstrate that this object is the sun (We are aware that today Quantum mechanics, the Schrodinger equation, and the de Broglie wavelength relation only use for subatomic scale and subatomic objects. But, in this article, we prove that quantum mechanics is also valid in astronomical scale and we will obtain the shape of Schrodinger equation and de Broglie wavelength relation in astronomical scale).

3. Wave Function of Solar System

As mentioned, a cosine and standing wave function, with the wavelength $\lambda = 0.6\ AU$ ($k = \frac{2\pi}{\lambda} = \frac{10\pi}{3}$), can predict the position of the planets in solar system. First we want to derive the phase constant ($\emptyset_0$) of this wave function. Any wave in which the variables x and t are entered as a combination of $kx \pm wt$ is a traveling wave [7]. For example, $\sin(kx - wt + \emptyset_0)$ is a traveling wave. Thus, a standing wave is in the form of $cos(wt)\, cos(kx + \emptyset_0)$ or $sin(wt)\, cos(kx + \emptyset_0)$ or $sin(wt)\, sin(kx + \emptyset_0)$ or $\cos(wt)\sin(kx + \emptyset_0)$. As mentioned, a cosine standing wave can predict the positions of planets. Therefore, the form of the standing wave of solar system must be either $sin(wt)\, cos(kx + \emptyset_0)$ or $cos(wt)\, cos(kx + \emptyset_0)$ (In the following, we choose one of these two forms). For the nodes of these two standing waves we have $cos(kx + \emptyset_0) = 0$. As mentioned previously, Mercury is on the second node of Solar system wave function (the second node corresponds to the phase $\frac{3\pi}{2}$ because $Cos\ \frac{3\pi}{2} = 0$). We have:

$$x_{Mercury} = 0.4\ AU \Rightarrow \psi(x_{Mercury}) = 0 \Rightarrow Cos(kx_M + \emptyset_0) = 0 \Rightarrow kx_M + \emptyset_0 = \frac{3\pi}{2} \xrightarrow{k=\frac{10\pi}{3}} \emptyset_0 = \frac{\pi}{6}$$

Having k and $\emptyset_0$, we can easily find the position of the other planets using the equation $kx + \emptyset_0 = \frac{\pi}{2}, \frac{3\pi}{2}, \frac{5\pi}{2}, \ldots\ldots, \frac{(2m-1)\pi}{2}$ (Where m is the node number). For example

$$kx_{Venus} + \emptyset_0 = \frac{5\pi}{2} \Rightarrow \frac{10\pi}{3}x_{Venus} + \frac{\pi}{6} = \frac{5\pi}{2} \Rightarrow x_{Venus} = 0.7\ AU$$

or

$$kx_{Earth} + \emptyset_0 = \frac{7\pi}{2} \Rightarrow \frac{10\pi}{3}x_{Earth} + \frac{\pi}{6} = \frac{7\pi}{2} \Rightarrow x_{Earth} = 1\ AU$$

$$kx_{Mars} + \emptyset_0 = \frac{11\pi}{2} \Rightarrow \frac{10\pi}{3}x_{Mars} + \frac{\pi}{6} = \frac{11\pi}{2} \Rightarrow x_{Mars} = 1.6$$

The distances of the other planets can also be calculated in the same way, which is quite consistent with experience. According to the above equation ($kx + \emptyset_0 = \frac{(2m-1)\pi}{2}$), Neptune is on the ninety-eighth node, which corresponds to the phase $\frac{195\pi}{2}$. Contrary to the TBL, which is not able to predict the distance of Neptune, our wave theory predicts the position of Neptune. Therefore, a cosine and standing wave function with $\emptyset_0 = \frac{\pi}{6}$ and $k = \frac{10\pi}{3}$ can be attributed to solar system. But what is the general equation of this wave function? As mentioned, the function of solar system must contain a component with the equation $cos(\frac{10\pi}{3}x + \frac{\pi}{6})$ and on the other hand, this wave must be standing so that the position of the nodes (planets) does not change. Therefore, as mentioned, the form of solar system wave function must be either $cos(\delta wt)\, cos(\frac{10\pi}{3}x + \frac{\pi}{6})$ or $sin(\delta wt)\, cos(\frac{10\pi}{3}x + \frac{\pi}{6})$. There is no difference between $cos(\delta wt)$ and $sin(\delta wt)$ Because we know from trigonometric identities that: $cos(\delta wt) = \sin\left(\delta wt + \frac{\pi}{2}\right)$. Therefore, we choose the function $cos(\delta wt)\, cos(\frac{10\pi}{3}x + \frac{\pi}{6})$ and then we will show that our choice is correct (δ is a constant number that we will derive its value). Since solar system has a certain size and is not infinitely wide, its wave function must be localized (a wave packet). If we consider an expression in the form $e^{-\gamma x^2}$ (which is a Gaussian function and plays the role of a wave envelope) in the final function of solar system, in such a case, the final equation is a localized wave or a wave packet[2]. The value of γ, which is a positive number, will be obtained in the following. Thus, the primary form of the wave function of solar system is as follows (equation 1) and the planets are on the nodes of this wave function (Fig. 1):

$$\begin{cases} \psi(x,t) = C\, cos(\delta wt)\, cos(\frac{10\pi}{3}x + \frac{\pi}{6})\; e^{-\gamma x^2} & x \geq 0 \\ \psi(x,t) = C\, cos(\delta wt)\, cos(\frac{10\pi}{3}x - \frac{\pi}{6})\; e^{-\gamma x^2} & x \leq 0 \end{cases} \quad (1)$$

In equation 1, γ, C and δ are constant values and we obtain their values in this article. This is an empirical equation which we will obtain it from mathematic methods in the next section.

[2] Although a Gaussian wave packet is also infinitely wide, but it is very localized.

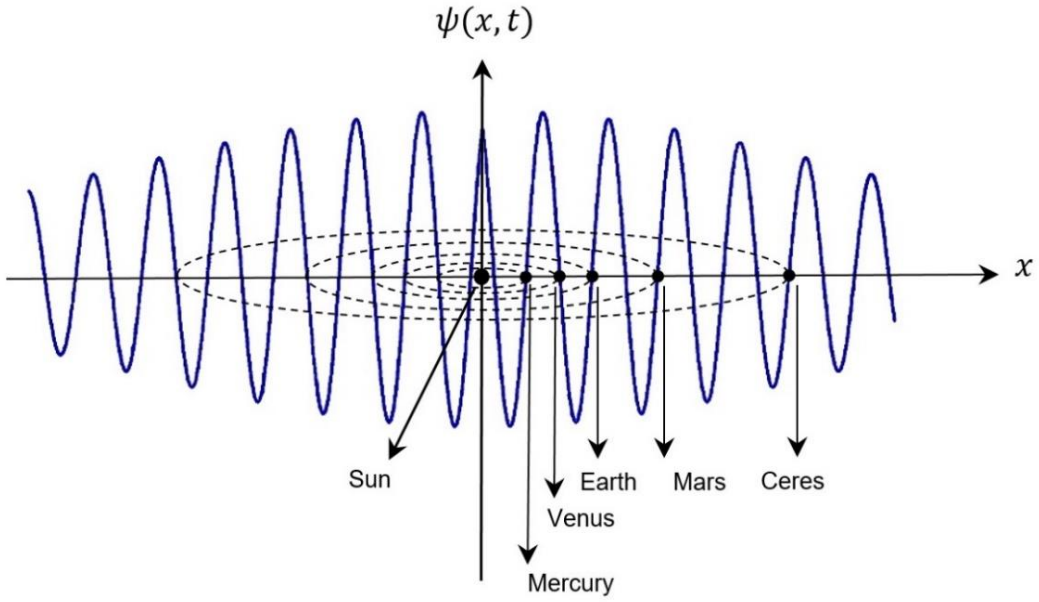

Fig. 1. Solar system standing wave packet with $\lambda = 0.6\ AU$ and $\emptyset_0 = \frac{\pi}{6}$. Diagram of $\psi(x,t)$ at the moment t = 0. The value of $\psi(0,0)$ equals $\sqrt{3}C/2$. This diagram is drawn by a certain value of C, δ and γ in equation 1, which we will obtain their value in this article. As you can see, the planets are on the nodes of the wave function. Jupiter, Saturn, Uranus, Neptune, and Pluto are on the nodes farther from the sun. The reason why there is no planet in some nodes will explained in the section 7: "Elliptical orbits and Isotropic Asteroid Belt". This is due to the unbalanced mass distribution in the protoplanetary disk of solar system.

In figure 1, the wave oscillates along the ψ axis over time. But the nodes and the anti-nodes do not move relative to each other along the x-axis. This does not mean that the wave packet is stationary in the space; it is just like passengers sitting on a train who do not move relative to each other but the train is moving relative to the rails. In the same way, solar system wave packet (equation 1) is a standing wave that rotates, along with solar system, around the center of the galaxy.

As you observed, function 1 could easily predicts the position of planets. In the continuation of the article, we will prove that this function is in the form of the real part of a solution of the Schrodinger equation (As you know, the solutions of the Schrodinger equation have two parts: Real and Imaginary) and that's why we can attribute it to an object like the sun. And in the section "Elliptical orbits and Isotropic Asteroid Belt" we will show that how we can arrive to the TBL from the protoplanetary disk, by oscillation of solar system wave function.

4. Single-Frequency Wave Packet

We obtained the equation of a single-frequency wave packet in the previous section, empirically (equation 1). But, a thought experiment [8] arrives us to this conclusion that a single-frequency wave packet cannot be existed. This thought experiment investigates the beat between two single-frequency waves. In this thought experiment, it is proved that only a wave with infinite spreading can be single-frequency. This means that a wave packet, which is localized, cannot be single

frequency. This experiment apparently has a logical and unambiguous face. but there is a very important problem about thought experiments. A thought experiment, even if is based on a logical process, may lead to wrong results. We prove this with an example. Here we use "counterexample" method (which is mathematic method) and with a counterexample we disproof of the generalization "All thought experiments lead to the right result". A well-known example is the famous experiment of Michelson and Morley about the velocity of light [9]. If you do the Michelson and Morley experiment in your mind[3], you will conclude that the velocity of light depends on the velocity of observer (velocity addition law). This was something that Michelson and Morley also expected. But when their experiments were performed in the real world, they concluded that the velocity of light is independent of the velocity of observer. This example shows that the intellectual and empirical results of an experiment may not be the same and therefore we cannot trust to the results of a thought experiment and we cannot use its results until it is not performed in the real world. This example fully proves that a thought experiment is meaningless because you cannot rely on its results and its results may be wrong. Obviously, this rule (Unreliability of the results of a thought experiment) also is true for the mentioned beat thought experiment. And therefore we cannot comment on the results of the beat experiment until it is performed. Which it means that we cannot comment on the existence or nonexistence of single-frequency wave packet. In addition, attention to the empirical equation 1 we have a single-frequency wave packet and therefore the beat thought experiment is contrary to observation and so is wrong.

In the next section, we will obtain equation 1 mathematically and we will show that the equation 1 is the real part of the solution of the Schrodinger equation.

5. Associated Wave Packet of Sun

In this section we will show that the equation 1 is exactly in the form of the real part of the solution of the Schrodinger equation that's why we can attribute it to an object like the sun. Base of calculations in this section is superposition principle. Consider a set of infinite number of flat matter waves $Ae^{i(kx-wt+\emptyset_0)}$, $Ae^{i(kx+wt+\emptyset_0)}$, $Ae^{i(kx-wt-\emptyset_0)}$ and $Ae^{i(kx+wt-\emptyset_0)}$ which move in the positive and negative directions of the x-axis; and assume that all of these waves are under the effect of potential $V(x)$[4]. These four groups of waves are all of possible form of flat matter waves. In such a case the angular frequency (w) of each of these matter waves is equal:

$$w = \frac{E}{\hbar} = \frac{1}{\hbar}\left(\frac{P^2}{2m} + V(x)\right)$$

[3] In fact, all experiments are initially a thought experiment. Some of them remain a thought experiment due to the human inability to perform the experiment in the real world, and some become real physical experiment.

[4] Since the solar system is under effect of gravity of Milky Way galaxy center; therefore here we investigated the superposition of matter waves which they are under the effect of potential.

Because, based on De Broglie theory, the energy of a matter wave is equal to the energy of associated particle of the wave i.e. E= $\frac{P^2}{2m} + V(x)$. As you know these four groups of waves with general equation $Ae^{i(kx \pm wt \pm \emptyset_0)}$ are the solution of the Schrodinger equation namely

$$i\hbar \frac{\partial}{\partial t}\psi(x,t) = -\frac{\hbar^2}{2m}\frac{\partial^2 \psi(x,t)}{\partial x^2} + V(x)\psi(x,t)$$

These waves sum together in space based on superposition principle. From these infinite number of waves we will show that the superposition of a part of these waves, which their angular frequency equals w_0 and their wave number is around the median of k_0 and between $k_0 + \Delta k/2$ and $k_0 - \Delta k/2$ and the amplitude changes of these waves is equal to $A(k) = (\frac{2\alpha}{\pi})^{1/4} e^{-\alpha(k-k_0)^2}$(which is a Gaussian function[5]), is in the form of equation 1.

First consider a set of infinite number of matter waves $Ae^{i(kx - wt + \emptyset_0)}$ which move in the positive direction of x-axis and their angular frequency equals w_0 and their wave number is around the median of k_0 and between $k_0 + \Delta k/2$ and $k_0 - \Delta k/2$ and the amplitude changes of these waves is equal to $A(k) = (\frac{2\alpha}{\pi})^{1/4} e^{-\alpha(k-k_0)^2}$. In such a case, the resultant of these waves, using the superposition principle, is a wave packet with equation 2 [10][11][12].

$$\psi_{total}(x,t) = \frac{1}{\sqrt{2\pi}} \int_{-\infty}^{\infty} A(k) e^{i(kx - w_0 t + \emptyset_0)} dk \qquad (2)$$

Where k means k_x. In equation $A(k) = (\frac{2\alpha}{\pi})^{1/4} e^{-\alpha(k-k_0)^2}$, α is a constant with a positive value and shows the width of the bell-shaped function $A(k)$. $(\frac{2\alpha}{\pi})^{1/4}$ is a normalization coefficient which is obtained by normalize of $A(k)$. Since equation 2 is derived from the superposition principle, it is the solution of the Schrodinger equation [12].

To obtain $\psi_{total}(x,t)$ from equation 2, we calculate the superposition of all of the waves in one moment, which we consider to be the origin of time ($t = 0$), and then we can obtain the net wave at any other time. We have:

$$\psi(x,0) = \frac{1}{\sqrt{2\pi}} \int A(k) e^{i(kx + \emptyset_0)} dk \qquad (3)$$

The above equation is the momentary image of the net wave. Multiply equation 3 by $e^{ik_0 x - ik_0 x}$. We have:

[5] In the Electromagnetic (EM) waves we cannot consider one w_0 for two or many waves in which their k is different from each other, because for all of the EM waves we have: $w = ck$ where c is the velocity of light. But for matter waves the issue is different. In the matter waves we have $w = \frac{\hbar k^2}{2m}$ [12]. As you can see w is the function of k and m. Therefore, it is possible to choose one value of w_0 for the waves in which their k is different from each other.

$$\psi(x,0) = \frac{1}{\sqrt{2\pi}} e^{i(k_0 x + \emptyset_0)} \int A(k) e^{i(k-k_0)x} dk \tag{4}$$

Considering $k' = k - k_0$, we have:

$$\psi(x,0) = (\frac{\alpha}{2\pi^3})^{1/4} e^{i(k_0 x + \emptyset_0)} \int e^{-\alpha k'^2} e^{ik'x} dk' \tag{5}$$

Using the variable transformation $k' - \frac{ix}{2\alpha} = q$ [10][11] and the Gaussian integral $\int_{-\infty}^{\infty} dq\ e^{-\alpha q^2} = \sqrt{\frac{\pi}{\alpha}}$, equation 5 can be calculated. After replacement and simplification, we reach the following final solution [10][11]:

$$\psi(x,0) = (\frac{\alpha}{2\pi^3})^{1/4} \sqrt{\frac{\pi}{\alpha}}\ e^{i(k_0 x + \emptyset_0)}\ e^{-\frac{x^2}{4\alpha}} = (\frac{1}{2\pi\alpha})^{1/4} e^{i(k_0 x + \emptyset_0)}\ e^{-\frac{x^2}{4\alpha}} \tag{6}$$

Lets check the normalization

$$\int_{-\infty}^{\infty} |\psi(x)|^2\, dx = \sqrt{\frac{1}{2\pi\alpha}} \int_{-\infty}^{\infty} e^{-\frac{x^2}{2\alpha}} dx = \sqrt{\frac{1}{2\pi\alpha}} \sqrt{2\alpha\pi} = 1$$

Given a normalized $A(k)$, we get the normalized $\psi(x)$.

Now, how is the time variation of equation 6? Let's go back to equation 2:

$$\psi(x,t) = \frac{1}{\sqrt{2\pi}} \int A(k) e^{i(kx - w_0 t + \emptyset_0)} dk = (\frac{\alpha}{2\pi^3})^{1/4} \int e^{-\alpha(k-k_0)^2} e^{i(kx - w_0 t + \emptyset_0)} dk$$

Substituting $e^{ik_0 x - ik_0 x}$ in the equation:

$$\psi(x,t) = (\frac{\alpha}{2\pi^3})^{1/4} e^{i(k_0 x + \emptyset_0) - iw_0 t} \int e^{-\alpha k'^2} e^{ik'x} dk'$$

This integral is similar to integral 5, which led to $\psi(x,0)$ (Equation 6). Therefore, we have:

$$\psi(x,t) = \psi_1(x,t) = (\frac{1}{2\pi\alpha})^{1/4}\ e^{i(k_0 x - w_0 t + \emptyset_0)}\ e^{-\frac{x^2}{4\alpha}} \tag{7}$$

$$e^{i\theta} = cos\theta + isin\theta \Longrightarrow\ Re\ \psi_1(x,t) = (\frac{1}{2\pi\alpha})^{1/4} cos(k_0 x - w_0 t + \emptyset_0)\ e^{-\frac{x^2}{4\alpha}} \tag{8}$$

Due to the presence of the factor $k_0 x - w_0 t$, equations 7 and 8 represent a traveling wave packet that propagates in the positive direction of the x-axis [7]. This means that the location of the nodes is not known. Due to the absence of t in $e^{-\frac{x^2}{4\alpha}}$ in equations 7 and 8, the wave packets in these equations does not spread.

Previous calculations was about superposition of the waves $e^{i(kx-w_0t+\emptyset_0)}$. Similarly, we use the recent trend to obtain the superposition of flat waves traveling in the negative direction of the x-axis, i.e. $Ae^{i(kx+w_0t+\emptyset_0)}$. If we do this, we get to equation 9:

$$\psi_2(x,t) = (\frac{1}{2\pi\alpha})^{1/4}\, e^{i(k_0x+w_0t+\emptyset_0)}\, e^{-\frac{x^2}{4\alpha}} \tag{9}$$

$$Re\ \psi_2(x,t) = (\frac{1}{2\pi\alpha})^{1/4}\, cos(k_0x + w_0t + \emptyset_0)\ e^{-\frac{x^2}{4\alpha}} \tag{10}$$

This equation shows a traveling wave packet that propagates in the negative direction of the x-axis.

Now we sum up the two equations 10 and 8 together to get the final wave.

$$Re\ \psi_{total}(x,t) = Re\ \psi_1 + Re\ \psi_2$$

Thus:

$$Re\ \psi_{total}(x,t) = (\frac{1}{2\pi\alpha})^{1/4}\, e^{-\frac{x^2}{4\alpha}}[cos(k_0x - w_0t + \emptyset_0) + cos(k_0x + w_0t + \emptyset_0)] \tag{11}$$

Using $cos\alpha + cos\beta = 2cos\frac{1}{2}(\alpha+\beta)cos\frac{1}{2}(\alpha-\beta)$ and $\cos(\theta) = \cos(-\theta)$ we obtain the equation of a standing wave packet.

$$\begin{cases}\alpha = k_0x - w_0t + \emptyset_0\\ \beta = k_0x + w_0t + \emptyset_0\end{cases} \Longrightarrow Re\ \psi_{total}(x,t) = 2(\frac{1}{2\pi\alpha})^{1/4}\cos(k_0x+\emptyset_0)cos(w_0t)e^{-\frac{x^2}{4\alpha}} \tag{12}$$

There is not the structure of $kx \pm wt$ in equation 12 so the ψ_{total} is a standing wave. As you observe, equation 12, which is the real part of a solution of the Schrodinger equation, is exactly the same as equation 1 for $x \geq 0$, which is solar system wave function. Is this similarity coincidental? No. Therefore equation 1 is the real part of a solution of the Schrodinger equation. It means that the Schrodinger equation and quantum mechanics are valid in astronomical scale. By comparing equation 12 and equation 1, we have

$$\delta = 1\ \ ,\ \ \gamma = \frac{1}{4\alpha} \quad and \quad C = 2(\frac{1}{2\pi\alpha})^{1/4}$$

If we put these values in equation 1, then we get the final equation of solar system wave function for $x \geq 0$:

$$Re\ \psi_t(x,t) = 2(\frac{1}{2\pi\alpha})^{1/4}\, cos(w_0t)\, cos(\frac{10\pi}{3}x + \frac{\pi}{6})\ e^{-\frac{x^2}{4\alpha}} \qquad x \geq 0 \tag{13}$$

Equation 13 is obtained by calculating the superposition of a set of infinite number of waves $Ae^{i(kx-w_0t+\emptyset_0)}$ and $Ae^{i(kx+w_0t+\emptyset_0)}$ that move in opposite directions to each other (pay attention to the + sign behind $\emptyset_0$). Now if we sum a set of infinite number of flat wave functions with the equations $Ae^{i(kx-w_0t-\emptyset_0)}$ and $Ae^{i(kx+w_0t-\emptyset_0)}$ (pay attention to the $-$ sign behind $\emptyset_0$) together, by following the path we have taken from equation 2 to equation 13, we reach the following relation;

$$Re\ \psi_t(x,t) = 2(\frac{1}{2\pi\alpha})^{1/4}\, cos(w_0 t)\, cos(\frac{10\pi}{3}x - \frac{\pi}{6})\ e^{-\frac{x^2}{4\alpha}}$$

Which is the same as equation 1 for $x \leq 0$. Therefore, the final form of solar system wave function (equation 1) is as follows:

$$\begin{cases} Re\ \psi(x,t) = 2(\frac{1}{2\pi\alpha})^{1/4}\, cos(w_0 t)\, cos(\frac{10\pi}{3}x + \frac{\pi}{6})\ e^{-\frac{x^2}{4\alpha}} & x \geq 0 \\ Re\ \psi(x,t) = 2(\frac{1}{2\pi\alpha})^{1/4}\, cos(w_0 t)\, cos(\frac{10\pi}{3}x - \frac{\pi}{6})\ e^{-\frac{x^2}{4\alpha}} & x \leq 0 \end{cases} \quad (14)$$

In this equation, the larger the α is, the more the width of wave packet, along the x-axis. We drew Fig. 1 by $\alpha = 10$. In this section we did not do anything strange. Rather, we have used only the superposition principle. We calculated the superposition of infinite number of flat matter waves with general equation $e^{i(kx \pm wt \pm \emptyset_0)}$ which their angular frequency equals w_0 and the wave number of these waves is around the median of k_0 and between $k_0 + {\Delta k}/{2}$ and $k_0 - {\Delta k}/{2}$ and the amplitude changes of these waves is equal to $A(k) = (\frac{2\alpha}{\pi})^{1/4} e^{-\alpha(k-k_0)^2}$ and they are under the effect of potential $V(x)$. There have been infinite number of flat matter waves in the early solar system which the superposition of a set of them made the wave function in figure 1. We will talk more about this in the section "Elliptical Orbits and Isotropic Asteroid Belt".

Here we demonstrated that solar system wave function (equation 1) is the real part of a solution of the Schrodinger equation. So, based on quantum mechanics, we can attribute it to an object in Solar system. The closest star to solar system is at a distance of 4.8 light-years, which is so far. And the biggest and heavyset object in solar system is sun. Therefore, the wave function of solar system can only belong to the sun. In the section "Elliptical orbits and Isotropic Asteroid Belt", we will discuss more about the formation of the solar system wave packet. De Broglie considered the wave nature for subatomic particles, and here we attributed the wave nature to celestial objects. Neither of these two actions is strange. Rather, they are truths that we must become accustomed to.

In this article, we proved that the Schrodinger equation is valid in astronomical scale; on the other hand, as you know, the Schrodinger relation is based on de Broglie equation ($\lambda = \frac{h}{mv}$). Therefore, the de Broglie equation is valid in astronomical scale[6]. But, according to the very large mass of sun, using the de Broglie relation the wavelength 0.6 AU will not obtain. So, instead of Planck constant we must choose another value for celestial objects, which is larger than h. We call this new value the Planck constant in Astronomy ($h_{Astronomy}$) abbreviated as h_A and we have: $\lambda_A = \frac{h_A}{P}$. In such a case, the Schrodinger equation in the astronomical scale can be written as follows:

[6] The Davisson–Germer experiment [14] is the confirmation of the existence of the de Broglie wave in subatomic scale and the regularity of the distances of the planets from sun (Titius-Bode rule) is the confirmation of the existence of the de Broglie wave in astronomical scale.

$$i\hbar_A \frac{\partial}{\partial t}\psi(x,t) = -\frac{{\hbar_A}^2}{2m}\frac{\partial^2\psi(x,t)}{\partial x^2} + V(x)\psi(x,t) \quad (15)$$

If we follow the path of proving the Schrodinger equation [13] and put the value $\hbar_A$ instead of $\hbar$, we reach equation 15. The Davisson–Germer experiment [14] is considered as the confirmation of existence of the de Broglie wave at the atomic scale, and the regularity of the distances of the planets from sun (Titius-Bode rule) is the confirmation of the existence of the de Broglie wave in astronomical scale. Moreover, for the celestial wave packet we will have $w = \frac{\hbar_A k^2}{2m}$.

6. Elliptical Orbits and Isotropic Asteroid Belt

In this section we will show that the nebular theory without our wave function theory is an incomplete theory and our wave function model must be attached to the nebular theory in order to explain the formation of the solar system.

The equation 14 in cylindrical coordinate is:

$$x = r\cos\theta \Rightarrow Re\,\psi(r,\theta,t) = 2\left(\frac{1}{2\pi\alpha}\right)^{1/4} cos(w_0 t)\, cos\left(\frac{10\pi}{3} r\, cos\,\theta + \frac{\pi}{6}\right) e^{-\frac{(r\cos\theta)^2}{4\alpha}} \quad (16)$$

Figure 2 is the shape of figure 1 in three dimensions based on equation 16:

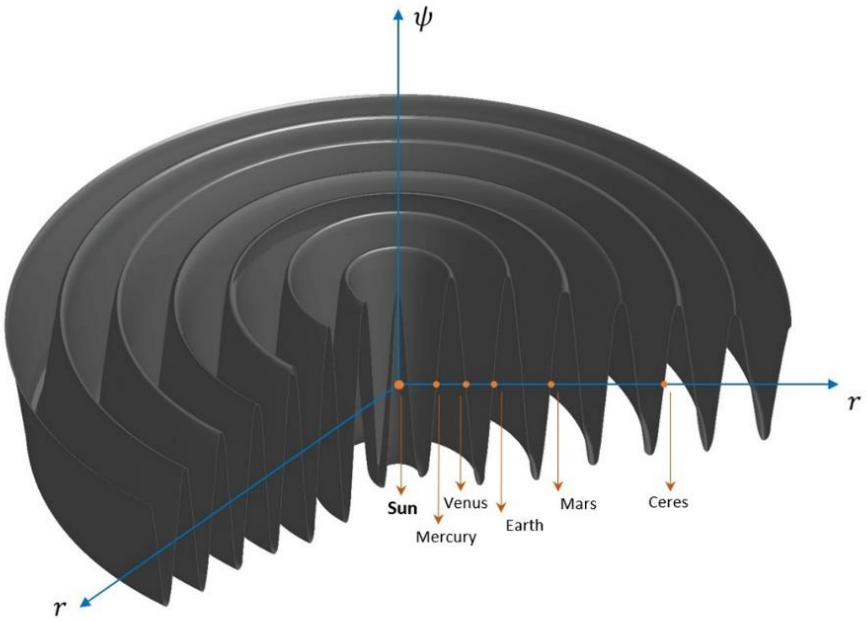

Fig. 2. The oscillation of solar system wave function in three dimensions. Here the wave function in Figure 1 is shown in three dimensions. Fig 2 is drawn in cylindrical coordinates using equation 16. Obviously, this wave function continues indefinitely, based on equation 1 (or equation 16). Because of existence the exponential factor in equation 16, the amplitude of the wave gradually decreases while we move away from the ψ-axis.

As you can see in Fig. 1 and Fig. 2, because of symmetry of equation 1, the orbits, created by the solar system wave function, are circle. But the real orbits of the planets are elliptic. The reason for

this is the existence of the inverse_square gravitational force of the sun[7]. As you know, the sun formed earlier than the planets [15][16][17]. Simultaneously with the formation of the sun, about 4.6 billion years ago [16], its wave function was also formed[8], and the oscillation of this wave function arranged and collected the gas and dust particles of the Protoplanetary disk in regular orbits (Titius-Bode orbit). Just like the standing wave patterns on the kettledrum head (Fig. 3) As you can observe in Fig.3, by a mechanical oscillator at the upper left of the photograph, the powder collects at the nodes [18]. As the same way, because of oscillation of solar system wave function, in some nodes of the wave function the gas and dust grains of protoplanetary disk agglomerated in the circular nodes (like figure 3) and then compressed due to collisions with each other[9] and formed larger grains, Planetesimals, Protoplanets and finally planets[10]. At the same time, the inverse_square force of the sun was at work, and changed the circular orbits to elliptical orbits. If you look closely, you will see that the mass distribution in the asteroid belt is similar to the powder ring in Figure 3.The mass distribution in the asteroid belt is uniform and isotropic, just like the powder ring in Figure 3, and this is another confirmation for our wave theory (In asteroid belt, Planet formation has stopped at the Planetesimals stage; And because of orbital resonances with Jupiter Protoplanet and planet was not formed [19]). Can a theory other than our wave theory explain the uniform and isotropic distribution of Planetesimals in the asteroid belt?

If solar system wave function did not exist; the planets might have been formed around the sun but the distance of planets from the sun was random and irregular. Without solar system wave packet, it is not possible to reach to the TBL from the protoplanetary disk. Thus, it seems that the existence of a standing wave in the solar system is undeniable. Therefore, the nebular theory becomes more complete by our wave function theory.

The reason why there is no planet in some nodes in figure 1 and 2 is due to the unbalanced mass distribution in the protoplanetary disk of solar system.

[7] We know from classical mechanics that the elliptic orbits of the planets (Kepler's first law) are the result of Newton's law of gravitation, which is an inverse_square relation

[8] The wave function of the solar system probably was formed either when the sun was a protostar or when the newborn sun was entered to the Main-sequence. The distance between these two phases is very short (less than 50 million years) [15] and both phases occurred before the formation of the planets. In both states, we have no idea how or why this wave function formed.

[9] "Collisions" were more like gentle touches. The particles were far too small to attract each other gravitationally at this point, they were able to stick together through electrostatic forces—the same "static electricity" that makes hair stick to a comb [20].

[10] Since the mass distribution in the Protoplanetary disk had not been uniform. During formation of the planets, in some nodes of the solar system wave function, less dusts were collected and in some nodes, more dusts were placed next to each other. Therefore, in some nodes a planet had been formed and in others it had not been formed.

Fig. 3. Standing wave pattern on a kettledrum head. One of many possible standing wave patterns on a kettledrum head, made visible by dark powder sprinkled on the drumhead. As the head is set into oscillation at a single frequency by a mechanical oscillator at the upper left of the photograph, the powder collects at the nodes. By the same way, due to the oscillation of the solar system wave function the dust grains and gas of the solar system protoplanetary disk were grouped in certain orbits.

7. What is Waving?

What is the nature of solar system wave function? As you know, since the solution of the Schrodinger equation is a complex function; It is meaningless to talk about what is waving [21][22]. But in this section we will show that the real part of the solution of the Schrodinger equation **probably** is the oscillation of Dark matter.

In this article, we showed that a standing wave oscillation had been effective in the formation of orbits of solar system planets and created the Bode rule. On the other hand, we know that the Dark matter interacts with the matters and affects them[11]. Therefore, it can be concluded that the standing wave oscillation in Fig. 1, with the equation 1, probably is the oscillation of Dark matter (Or dark matter is one of the candidate for the nature of solar system wave function). On the other hand, the equation 1 is the real part of a solution of the Schrodinger equation. Therefore, the real part of the solution of the Schrodinger equation is the oscillation of Dark matter. Of course, the Spacetime also interacts with matter and affects it. But we cannot consider the oscillation of Spacetime as the wave of the solar system. Because in such a case the curvature of Spacetime lines in figure 2 causes the planets to move along the r-axis. I think this article could give scholars new ideas about dark matter. Of course, there is another possibility. This wave may not be dark matter. It might be something we are not familiar with.

[11] In addition to gravitational interactions, dark matter may also have elastic collision (like collision between drumhead and dark powder particles in fig 3) with baryonic matter (namely objects made with protons, neutrons, and electrons like gas-dust particles in protoplanetary disk)

8. Solar System Wave Function and the Other Theories

Up-to-date astronomy books, such as the very famous book: ‘’Astronomy’’ by Professor Michael Zeilik (9th edition, 2002), usually list seven observational features for the solar system, which one of them is the TBL [23]. To compile our article, we read a lot about the attempt and work of previous scholars. We explain here the features of the existing theories in the language of a good book namely ‘’ The Titius-Bode Law of Planetary Distances’’ by Professor Michael Martin Nieto (1972) [24]. Due to curiosity of Mr. Nieto about the reason for TBL (As he says in the Foreword of his book), he carried out a comprehensive study about theories that had been formed until 1972. In this book, he investigates about 13 theories, which are about reason of TBL. We read in this book at the beginning of chapter 11: ((. . . the theories about Bode law can roughly be categorized as either: a) electromagnetism theories b) gravitational theories c) nebular theories . . . Unfortunately, many of the theories that we will review are "theories" and "Laws" in large part due to assumptions or arguments of possibility rather than by calculations that predict definite and unambiguous results . . . Too often the Titius-Bode Law has been discussed in terms of some mechanism which could conceivably produce the Law if all other physical effects could be ignored. Sad to say, that is not the type of physical universe with which we are dealing. Thus, one should be aware of the fact that any claim that a particular theory of the solar system is correct since it explains the Titius-Bode Law is not valid because, as of yet, no theory has properly explained this Rule. What can be said of some theories is that they are compatible with and indicative of a Titius-Bode Law, but not very much more.)) [25]. For example, In his three article, Hannes Alfven hypothesized that if he consider the original solar dipole moment 100000 times larger than at present and ignore the angular momentum in the early solar system [26] He could explain the mass distribution in the solar system. Or Hendrick Petrus Berlage, in his theory, assumed that the Sun emitted positive ions and negatively charged, solid particles that had condensed in the solar atmosphere. Berlage then further hypothesized that all the planet rings were formed a constant distance $d = 0.4\ AU$ further out from the ion rings (because of the addition of momentum to the growing Planetesimals via radiation pressure) [27]. But in our article is not any simplification or assumption. Our paper, without eliminating the physical parameters of solar system, justifies the Bode law and elliptical orbits. The oscillation of solar system wave function put up the gas-dust particles of protoplanetary disk in the circular orbits (nodes) just like Figure 3. In the first four pages of the article, we simply arrived to the TBL using wave theory. The important point is that none of the 13 theories examined in Professor Nieto's book easily reach the TBL. And most of them give this law or the other shape of it by approximating. Of course using a lot of assumptions and simplifications. None of these theories is satisfactory.

It seems that no specific work has been done on the cause of the TBL since 1970. In Professor Peter Lynch's 2003 article, we read:’’ Despite the distinguished part the Titius–Bode law has played in the evolution of our knowledge of planetary dynamics, no theoretical explanation of it has been advanced that has found general acceptance.’’[28]

In addition, some calculations and attempts were made which showed that TBL was a matter of chance. But in 2003, Professor Peter Lynch denied that it was a coincidence: ‘’ . . . this conclusion

is unsafe, and that the possibility that the observed regularity in the patterns of the planetary and satellite systems has some physical explanation is still open.’’[28].

9-1. The new Atomic model

It makes sense if we want to generalize our theory about solar system to the subatomic world. In this section, we present a new atomic model based on the model of the solar system wave function namely Fig. 2. Our atomic model explains why the Bohr atomic orbits are quantized. Niels Bohr could not explain this issue. Based on this model, the main spectrum of the hydrogen atom, the secondary spectrum, the normal Zeeman effect, and the other phenomena will be explained in a completely understandable way. Some of the atomic models are shown in Fig. 4.

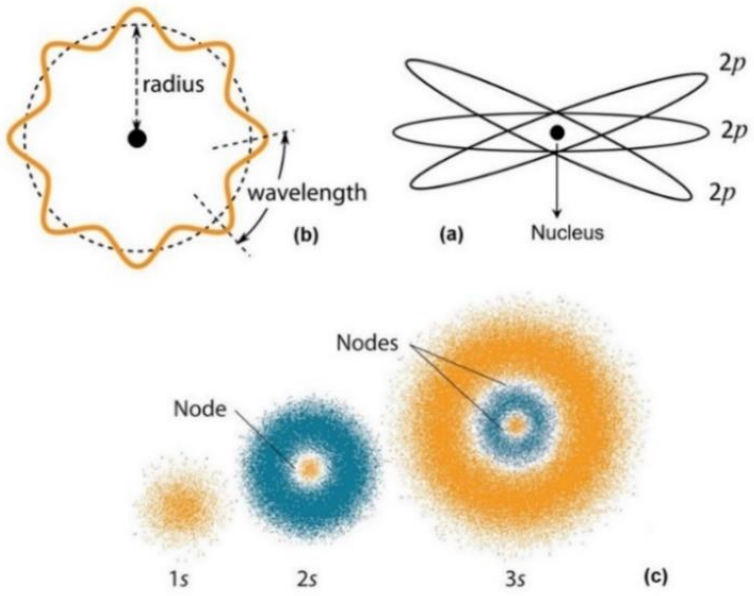

Fig. 4. Some of the atomic model. This figure shows three atomic models: **a).** Bohr-Sommerfeld atomic model: In this model, as you can see, subshells have space orientation. In this model, the horizontal $2P$ subshell is in the same plane as the $1S$ and $2S$ subshells. $1S$ and $2S$ subshells are not shown in this figure. **b).** De Broglie atomic model and **c).** the Schrodinger atomic model. In this figure Schrodinger’s S orbitals are shown. According to Max Born probability theory, the electron can be found in the distance between the nodes in the Fig. 4c. Other atomic models, such as the Rutherford or Thomson atomic models, are not shown in this figure.

Figure. 5 shows our atomic model, which we call the "New Atomic Model". To arrive to figure 5, we used the same method as at the beginning of this article. The Bohr atomic model is a successful model which its orbits are at x_1 = 0.53Å, $x_2 = 4x_1$, $x_3 = 9x_1$, etc. In order to be able to attribute a standing wave to Bohr model, our wavelength must be equal to $2x_1 = 1.06$ Å. Suppose the first orbit of the new atomic model is the first orbit in the Bohr atomic model, namely $x_1 = 0.53$ Å. The first orbit in our model is equivalent to the first node and the first node means $\emptyset = \frac{\pi}{2}$ because $Cos\ \frac{\pi}{2} = 0$. In such a case we have:

$$x_1 = 0.53\,\text{Å} \Rightarrow \psi(x_1) = 0 \Rightarrow cos(kx_1 + \emptyset_0) = 0 \Rightarrow kx_1 + \emptyset_0 = \frac{\pi}{2} \xrightarrow{k=\frac{2\pi}{1.06}} \emptyset_0 = -\frac{\pi}{2}$$

In the same way as the reasonings at the section 3, the final form of "hydrogen atom wave function" is equal to:

$$\begin{cases} Re\,\psi(x,t) = 2(\frac{1}{2\pi\alpha})^{1/4}\, cos(w_0' t)\, cos(5.92x - \frac{\pi}{2})\; e^{-\frac{x^2}{4\alpha}} & x \geq 0 \\ Re\,\psi(x,t) = 2(\frac{1}{2\pi\alpha})^{1/4}\, cos(w_0' t)\, cos(5.92x + \frac{\pi}{2})\; e^{-\frac{x^2}{4\alpha}} & x \leq 0 \end{cases} \qquad (17)$$

The equation 17 in cylindrical coordinate:

$$x = r\cos\theta \Rightarrow\; Re\,\psi(r,\theta,t) = 2(\frac{1}{2\pi\alpha})^{1/4}\, cos(w_0' t)\, cos(5.92r\cos\theta - \frac{\pi}{2})\; e^{-\frac{(r\cos\theta)^2}{4\alpha}} \qquad (17-a)$$

In equation 17, we consider the angular frequency equal to w_0' that not to be confused with w_0 in equation 14. Figure 5 is drawn in cylindrical coordinate. In the same way in Section 5, we can show that the equation 17 is the real part of the solution of the Schrodinger equation.

The first node of the associated wave packet of the hydrogen nucleus is at r_1 = 0.53Å and the second node is at $r_2 = 2r_1$, and Third at $r_3 = 3r_1$, etc. In the new atomic model we have: $r_n = nr_1$, and in the Bohr model we have $r_n = n^2 r_1$. This means that the orbit number n in the Bohr model is the orbit number n^2 in the new atomic model. For example, the second orbit in the Bohr model is the fourth orbit in the new atomic model (Fig. 6). In figure 5 the electron rotates on the first node of the associated wave packet of the nucleus (just like rotation of planets in Fig. 2). This orbit, like the orbits of the planets in the solar system, is slightly elliptical due to the inverse-square coulomb force of the nucleus. The protuberances in the nucleus wave function are the oscillation of dark matter. As mentioned in the section "Elliptical orbits and Isotropic Asteroid Belt", the role of the oscillation of the wave function is to prevent an electron from being placed between the nodes. In the new atomic model, the formation of an atom (for example, a hydrogen atom) is such that the electron approaches the proton and is placed in the first node of the proton associated wave packet. The proton associated wave packet prevents the electron from being placed in the distance between the nodes. Due to the Coulomb force, the electron begins to rotate around the nucleus on an elliptical orbit. In this atomic model we use Bohr's assumptions and assume that the electron does not radiate while it orbits about the nucleus [2]. In this model, like the Bohr model, the spectral lines of the elements are caused by the jump of electrons from the higher orbits to the lower orbits [2], which we will discuss in the next section about it. In fact, the Bohr atomic model is a subset of the new atomic model.

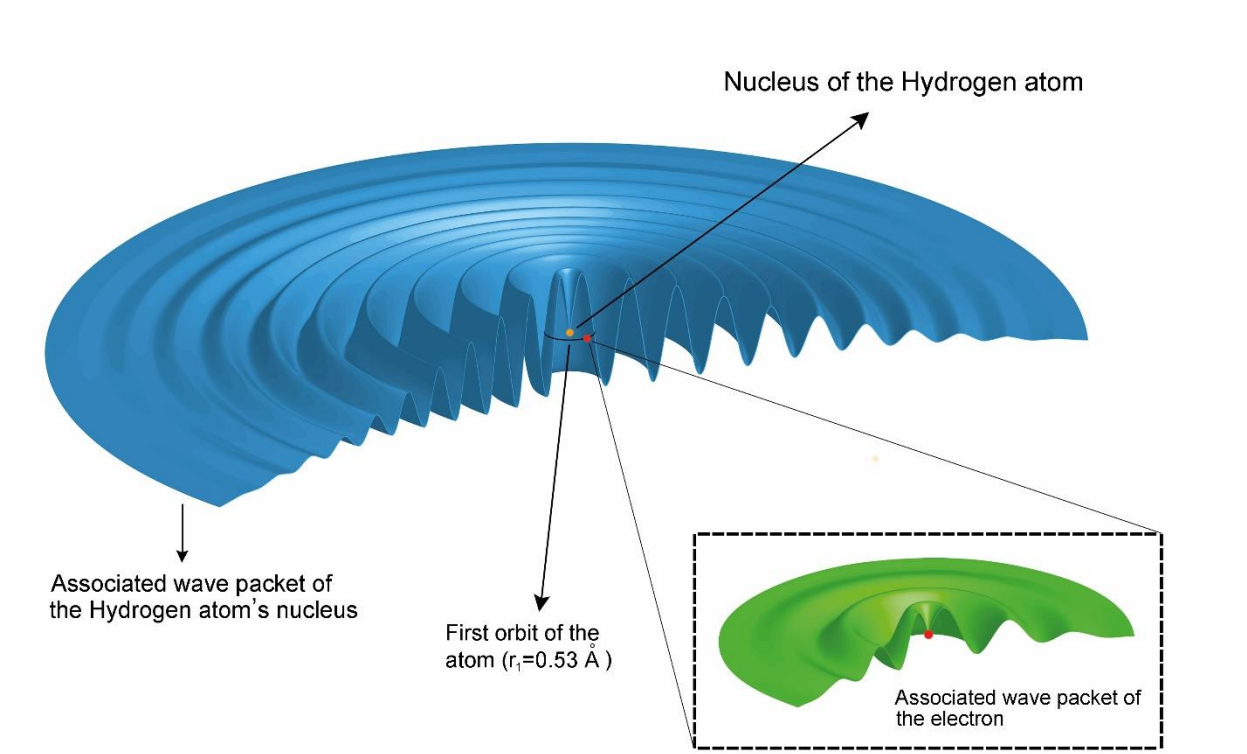

Fig. 5. The New atomic model. Diagram of $\psi(x,t)$ at the moment t = 0 based on equation (17-a) (blue wave packet). In this figure, associated wave packet of nucleus and associated wave packet of the electron are shown at t = 0. In this figure, the electron and its associated wave rotate about the nucleus of hydrogen atom. The second and the other orbits are not shown in this figure. We consider the wavelength of the nucleus wave packet to be $2r_1$ ($r_1 = 0.53$Å). If we consider the first orbital velocity of electron based on the Bohr model $v_1 = \frac{1}{137}c$, in such a case the wavelength of associated wave packet of electron in the first orbit of hydrogen, based on de Broglie equation ($\lambda = \frac{h}{mv}$), is 3.3 Å (Although, no one has ever measured the velocity of the electron in the first orbit of the hydrogen atom with a laboratory device or method; But $v_1 = \frac{1}{137}c$ is an empirical value. If v_1 does not have this value, then the precise value of Rydberg constant is not obtained from the Bohr model). There is no matter if the wavelength of associated wave of electron is larger than or less than the wavelength of the associated wave of the nucleus.

In figure 5, The nucleus wave function is plotted using equation 17 with $\alpha = 7$ and $\lambda = 2r_1 = 1.06$ Å or $k = 5.92$. And the electron wave function with $\lambda = 3.3$ Å or $k = 1.9$ and $\alpha = 7$. The new atomic model includes both the Schrodinger wave function and the Bohr atomic model inside. In fact, Niels Bohr and Schrodinger each were achieved to a piece of reality, and Figure 5 is probably total of reality and the final atomic model.

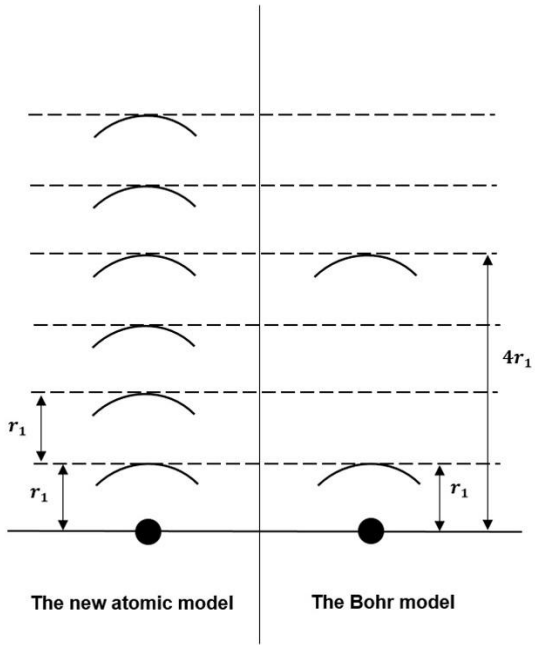

Fig. 6. The new atomic model compared to the Bohr model. For example, the second orbit in the Bohr model is the fourth orbit in the new atomic model.

Regarding Figure 5, we said that the associated wave packet of a particle is dark matter. Dark matter has mass. The mass we measure for elementary particles, such as electron and proton, with different ways is actually the mass of the particle itself and its associated wave packet. Therefore, because the proton is heavier than the electron, its wave packet probably is denser and heavier than the electron wave packet.

In the next section, first we will investigate the motion of electron around the nucleus in a hydrogen atom ($_1^1H$) and then, based on the diagram of the first ionization energy of the elements, present our general atomic model and we achieve interesting results.

9-2. The Atomic Hydrogen Model

We know from mechanics that a mass or an electric charge that is affected by a central force moves on an ellipse which its orbital eccentricity is

$$e = \sqrt{1 + \frac{2EL^2}{mK^2}} \tag{18}$$

Where E is the mechanical energy of the mass m, L is the orbital angular momentum and $K = k_e q_1 q_2$ or $K = GMm$ [29]. Semi-major axis of this ellipse is

$$a = -\frac{K}{2E} \tag{19}$$

And semi-minor axis is $b = a\sqrt{1 - e^2}$. The area of this ellipse is $A = \pi ab$ [29].

In the motion under the effect of central force L is a constant. And in our new atomic model because of existence of associated wave packet of nucleus, L is also quantized. The amount of L for the first orbit of hydrogen atom is $L_{1H} = Constant$. We have:

$$L_{1H} = Constant \ , \ K = k_e e^2 \Longrightarrow e_{1H} = \sqrt{1 + \frac{2E_{1H}L_{1H}^2}{m_e(k_e e^2)^2}} \tag{20}$$

E_{1H} is 13.6 eV, based on diagram of first ionization energy. Therefore all of the values in equation 20 are certain values and thus e_{1H} (namely the orbital eccentricity of first orbit of hydrogen atom) has a certain value. The semi-major axis equals

$$a_{1H} = -\frac{K}{2E_{1H}} \Longrightarrow a_{1H} = -\frac{k_e e^2}{2E_{1H}} = 0.528 \text{ Å} \tag{21}$$

This number is the same radius of the first orbit of the Bohr atom. The semi-minor axis is equal to:

$$b_{1H} = a_{1H}\sqrt{1 - e_{1H}^2} \tag{22}$$

In such a case, the area of orbit equals : $A_{1H} = \pi b_{1H} a_{1H}$. The orbit of electron is a current loop and therefore the orbital magnetic dipole moment for hydrogen atom is equal to:

$$\boldsymbol{m}_{1H} = I\boldsymbol{A}_{1H} \tag{23}$$

Where I is electric current [30]. In the new atomic model, the direction of the orbital magnetic dipole moment is perpendicular to the plane of the orbit. The dependence of the orbital magnetic dipole moment to the area of the orbit of electron is a very important issue that helps us to justify the normal Zeeman effect. In the following sections, we consider a few subshells for each main orbit, which the areas of these subshells are different from each other. This difference is the cause of difference in the value of $\boldsymbol{m}$, which helps us to justify the normal Zeeman effect. This method is different from Bohr-Somerfield method [31] in old quantum theory. In their model, the normal Zeeman effect is justified by difference in the space orientation of the subshells (Fig. 4a). But in our model, all of the subshells are in the same plane and the difference is in the areas.

9-3. Many-Electron Atoms

The diagram of the first ionization energy is a very valuable diagram that arrived scientists to many results (Fig. 7). It was by investigation of this diagram that they realized the existence of subshells, the order of subshells filling, and many other results. For example, this diagram shows that in the first shell is not P subshell, or d subshell does not exist in the first and second shells, or in another example, this diagram shows that $4S$ subshell fills earlier than $3d$.

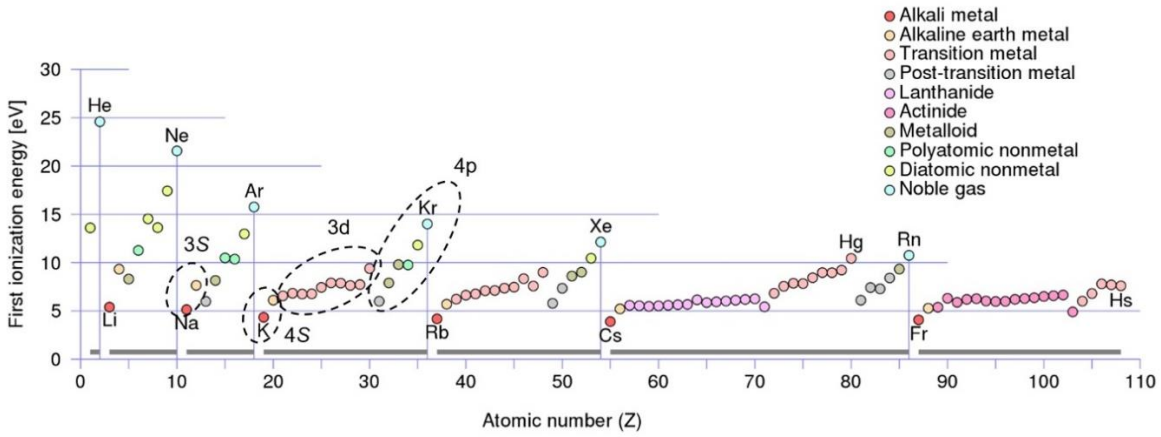

Fig. 7. The diagram of the first ionization energy.

In the new atomic model, according to the diagram of the first ionization energy and similar to the Bohr-Somerfield model, for each n layer, located at the distance $r_n = nr_1$; we consider the S, P, d, f and g subshells. These are circular and elliptical orbits that have not orientation, unlike the Somerfield model; and all of them are in the same plane and the difference is in their area (the reason for the formation of these subshells can be attributed to the quantized nucleus electric charge and electron charge). The orbital eccentricity and area of these subshells cannot be calculated (except for the hydrogen atom), but we assume that the area of the subshells is not equal. The difference in the area of the subshells cause a difference in the value of the ***m*** vector, which causes the occurrence of normal Zeeman effect. For example, the Neon atom has five subshells in the new atomic model. One subshell is $1S$, another $2S$ and three $2P$. All of these subshells are in the same plane, and in each of these subshells, based on the Pauli Exclusion Principle, only two electrons rotate. Here we consider a numeric index for each of the similar subshells. For example consider $2P$ subshells. we will have $2P_1, 2P_2$ and $2P_3$.

9-4. Quantum jumps and Spectral Lines of the Atomic Hydrogen

Before the Bohr atomic model, scientists did not know whether the particles in a hydrogen lamp were molecules or atoms. Because of justification of spectral series such as the Ballmer, Lyman, and Paschen series, by the Bohr atomic model, they understood that most of the particles inside the hydrogen lamp are atoms. But in the hydrogen spectrum, there are other lines besides the main spectrum lines (namely Ballmer, Lyman, …. series.) [3][4][5][6], which are called secondary spectral lines. These lines are not predicted by the Bohr atomic model. By 1922, 750 number of these lines were discovered between H_α and H_β [4] (H_α and H_β are the first and second frequencies of the Ballmer series). Some physicists have linked secondary lines to impurities in the hydrogen lamp [3], and some have attributed them to hydrogen molecules in the lamp [3]. But all this was just speculation. Our theory considers a large part of these lines to be related to hydrogen atoms and theoretically predicts their existence and gives us their wavelengths. Today, these lines are known as the molecular spectrum of hydrogen [32][33], which this is based on Merton's article [3]. Merton in his article and in the section "Experimental Results" proved in a very vague way

that two groups of the secondary spectrum lines are related to hydrogen molecules and finally concluded that: "it is probable that the whole of the secondary spectrum is due to the hydrogen molecule". But we show that this is wrong, and only a part of these lines are related to hydrogen molecules.

In the Bohr atomic model, the lines of the emission and absorption spectrum of hydrogen atom are the result of quantum jumps. We use the same assumption in the new atomic theory. Consider Figure 6. As we said, if the Bohr model has n orbits, the new atomic model has n^2orbits. For example, the second Bohr orbit is the fourth orbit in the new atomic model (Fig. 6). Based on this, for example, Ly_α in the Lyman series, which equals ν_{21} in the Bohr model, is equal to ν_{41} in the new atomic model. Since the number of orbits in the new atomic model is more, we should expect more quantum jumps and consequently more emission lines in the hydrogen spectrum. For example, according to Fig. 6, in the new atomic model, we should be able to observe $\nu_{21}, \nu_{32}, \nu_{31}, \nu_{51}$, ... and many other frequencies, in addition to the lines predicted by the Bohr atomic model. For example, ν_{31} in the new atomic model equals

$$h\nu_{31} = E_3 - E_1 \xrightarrow{E_H=\frac{-\mu k_e e^2}{2m_e r}} \nu_{31} = \frac{1}{1+\frac{m_e}{M_P}}\frac{k_e e^2}{2h}\left(\frac{1}{r_1}-\frac{1}{3r_1}\right) = 3.35\times 10^{15}\times\frac{2}{3} \Longrightarrow$$

$$\therefore \nu_{31} = 2.23\times 10^{15}\ Hz \Longrightarrow \lambda_{31} = 1340\ \text{Å}$$

In the above calculations we used from equation $E_H = \frac{\mu}{m_e}E_\infty = \frac{-\mu k_e e^2}{2m_e r} = \frac{1}{1+\frac{m_e}{M_P}}\frac{k_e e^2}{2r}$ instead of $E_\infty = \frac{-k_e e^2}{2r}$ [34][35]. The equation $E_\infty = \frac{-k_e e^2}{2r}$ is the equation of energy of electron when the mass of nucleus is infinite. In the above equation μ is reduced mass. The Bohr atomic model do not predict the wavelength $\lambda_{31} = 1340$ Å. The observation of this wavelength in the hydrogen spectrum is a strong confirmation for the new atomic theory. As another example, based on the new atomic model, we have:

$$h\nu_{114} = E_{11} - E_4 = \frac{1}{1+\frac{m_e}{M_P}}\frac{k_e e^2}{2}\left(\frac{1}{4r_1}-\frac{1}{11r_1}\right) \Longrightarrow \nu_{114} = 0.53\times 10^{15}\ Hz \Longrightarrow \lambda_{114} = 4640\ \text{Å}$$

This ray is in the visible spectrum region and we should be able to observe it. Another examples are:

$$h\nu_{104} = E_{10} - E_4 \Longrightarrow \lambda_{104} = 4925\ \text{Å} \qquad and \qquad \lambda_{84} = 5980\ \text{Å}$$

These two wavelengths along with the previous wavelength can be easily seen in Fig. 8. This diagram shows the spectrum of a deuterium arc lamp, instead of a hydrogen lamp. The Deuterium lamp mostly used in spectroscopy, because it provides more intensity at shorter wavelengths and in the ultraviolet region. The wavelengths displayed in the deuterium spectrum are exactly the same as the wavelengths of the hydrogen spectrum with a very slightly shift toward shorter

wavelengths[12] [35] (this is due to the very small difference between Rydberg constant for deuterium and hydrogen [35]). In Fig. 8, D_α and D_β are consecutive wavelengths of the Ballmer series. The number of the secondary lines is very large both at short wavelengths and at long wavelengths.

As mentioned, our atomic model (Fig. 5) is based on equation 17. In this equation, the exponential factor is never zero, and therefore the infinite number of orbits can be considered around the nucleus of each atom. By moving away from the nucleus according to equation 17, the effects of the Coulomb force of the nucleus decreases; Therefore, in distant orbits, the electron is practically not bound to the nucleus.

In addition to the new atomic model, some secondary lines are definitely related to hydrogen molecules or impurities inside the lamp.

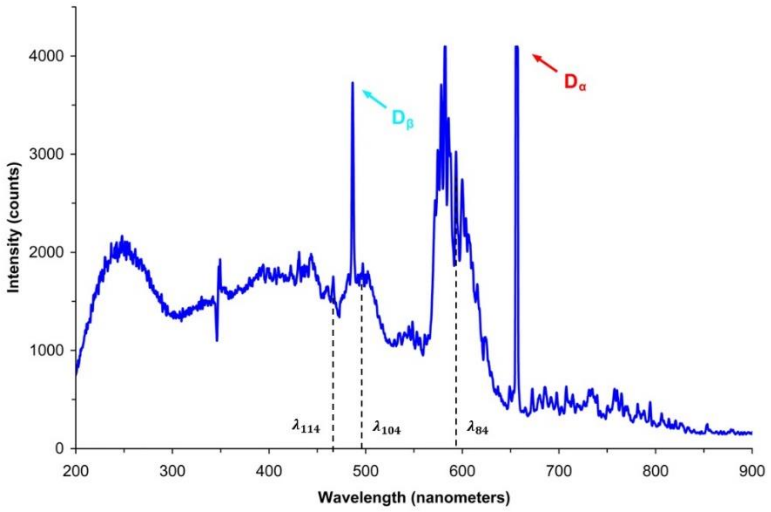

Fig. 8. The spectrum of the deuterium lamp. In this diagram, the position of the wavelengths is shown slightly approximately.

9-5. The Normal Zeeman Effect

The splitting of spectrum lines in the presence of an external magnetic field, or the normal Zeeman effect (NZE), was discovered by Zeeman in 1896. In the years that followed, Sommerfeld, who justified the fine structure by considering elliptical subshells for each orbit [36], assumed that each of these subshells has a different space orientation and all are not in the one plane [37]. For example, the three *P* subshells in the second orbit have three orientations (Fig. 4a). As mentioned, in the new atomic model we considered all of the subshells in one plane and assume that these subshells have different areas. Because of difference between these areas the orbital magnetic dipole moments of subshells ($\boldsymbol{m}$) will be different from each other, based on equation 23.

[12] This difference is not appearing until three digits after the decimal point

In the following, based on this point, we will explain NZE, in the usual way of proving the NZE in the old quantum mechanics [31]. The difference is that now the cause of the difference in the amount of $\boldsymbol{m}$ is the area of the subshells, not their space orientation.

Consider the third orbit of an atom and its nine subshells and assume that the area of these subshells are as shown in table 2.

Subshell of the third orbit	$3S$	$3P_1$	$3P_2$	$3P_3$	$3d_1$	$3d_2$	$3d_3$	$3d_4$	$3d_5$
Area of subshell($A_{subshell}$)	$20A_0$	$18A_0$	$20A_0$	$22A_0$	$16A_0$	$18A_0$	$20A_0$	$22A_0$	$24A_0$

Table. 2. The areas of third orbit's subshells. Here A_0 is a unit value. In this table the areas of $3S$, $3P_2$ and $3P_3$ is equal. But there is no problem about this. $3S$ is a circle; $3P_2$ is an ellipse and $3P_3$ is a more elongated ellipse.

In such a case, the difference in the energy levels in the presence of the magnetic field is obtained from the following equation:

$$\Delta E_m = -\boldsymbol{m}_{subshell} \,.\, \boldsymbol{B} = -I\boldsymbol{A}_{subshell} \,.\, \boldsymbol{B} \tag{24}$$

Where $\boldsymbol{m}_{subshell}$ is the orbital magnetic dipole moment of each subshell. If we assume that the direction of $\boldsymbol{B}$ is perpendicular to the orbital plane (or in the direction of $\boldsymbol{A}_{subshell}$), in such a case we have:

$$\Delta E_m = -IA_{subshell}B \tag{25}$$

We want to investigate the transition between d and P states in the presence of a magnetic field. When the magnetic field is zero, the energy of the d state is E_d (for all five d subshells) and the energy of the P state is E_P (for all three P subshells) and because of transition between d and P a photon will be emitted by energy: $h\nu_0 = E_d - E_p$. When the field is turned on, the d state splits into five equally spaced magnetic sublevels, and the P state splits into three equally spaced magnetic sublevels. According to the Table 2 the difference in energy between any two adjacent magnetic sublevels being $\Delta E_m = I2A_0B$. Here we should consider the selection rules. We should assume that the transitions between the subshells follow the rule $\Delta l = \pm 1$; Where the values of l are based on the table. 3:

$l = 0$	$l = 1$	$l = 2$	$l = 3$	$l = 4$
S	P	d	f	g

Table. 3. The subshells and their numbers. Here we use the l sign only because of the historical aspect of the subject, and its connection with Schrodinger mechanics and angular momentum is by no means intended in this section. We can use any other sign.

$\Delta l = \pm 1$ means that the transition from d to P is allowed but from d to S is forbidden. And we also should consider a selection rule for changing area of the subshells. we have:

$$\Delta A_l = 0 \quad or \quad \pm 2A_0$$

That is, only those transitions are allowed in which either A_l does not change or changes by $2A_0$. For changes of n (principal quantum number) any value is allowed. Authorized transitions are shown in Fig. 9.

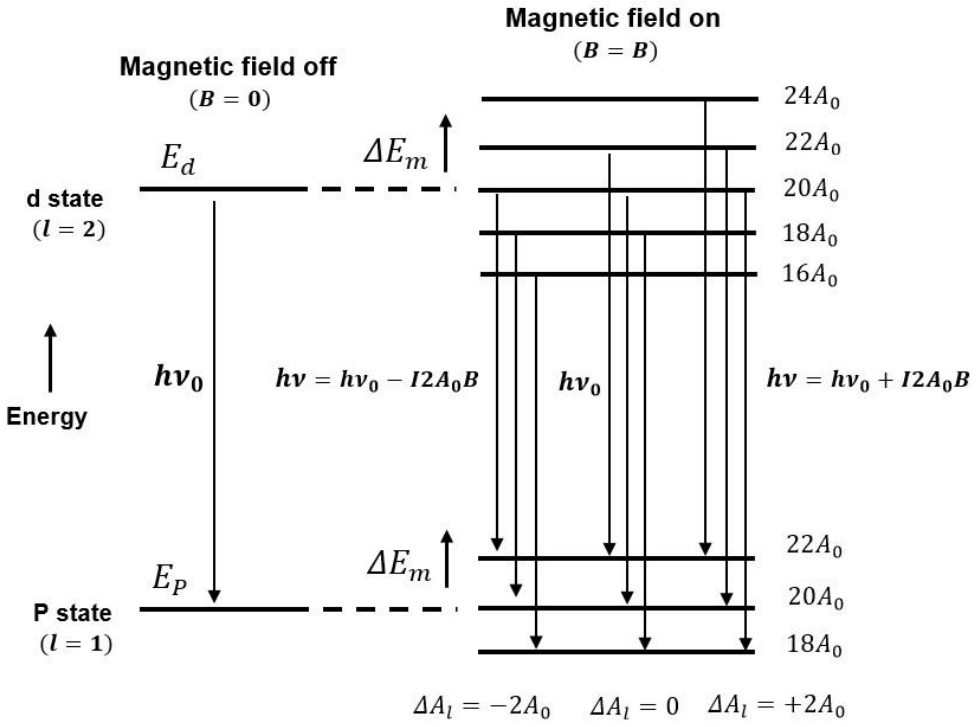

Fig. 9. Schematic illustration of normal Zeeman effect. Energy levels and spectra of $d \longrightarrow P$ transition: (left) zero magnetic field. (right) nonzero magnetic field.

We have:

$$\Delta A_l = 2A_0: \qquad h\nu = h\nu_0 + \Delta(\Delta E_m) \Longrightarrow h\nu = h\nu_0 + I2A_0B \Longrightarrow \nu = \nu_0 + \frac{I2A_0B}{h}$$

$$\Delta A_l = 0: \qquad h\nu = h\nu_0 + \Delta(\Delta E_m) \Longrightarrow h\nu = h\nu_0 \Longrightarrow \nu = \nu_0$$

$$\Delta A_l = -2A_0: \qquad h\nu = h\nu_0 + \Delta(\Delta E_m) \Longrightarrow h\nu = h\nu_0 - I2A_0B \Longrightarrow \nu = \nu_0 - \frac{I2A_0B}{h}$$

Thus, each line in the emission spectrum splits into three lines by an external magnetic field. As we said, we used the same common method of proving the NZE [31] here. The difference is that

here, instead of space orientation of the orbits, the difference in the area of the orbits causes the lines to split. This description of the NZE is easier than the Sommerfeld model.

The above relations were obtained in the situation that $\boldsymbol{B}$ was in the direction of $\boldsymbol{A}$. If $\boldsymbol{B}$ and $\boldsymbol{A}$ have a θ angle with each other, then in the two equations of above relations we will have $Cos\theta$:

$$\Delta A_l = 2A_0: \qquad h\nu = h\nu_0 + I2A_0BCos\theta \Longrightarrow \nu = \nu_0 + \frac{I2A_0B}{h}Cos\theta$$

$$\Delta A_l = 0: \qquad h\nu = h\nu_0 \Longrightarrow \nu = \nu_0$$

$$\Delta A_l = -2A_0: \qquad h\nu = h\nu_0 - I2A_0BCos\theta \Longrightarrow \nu = \nu_0 - \frac{I2A_0B}{h}Cos\theta$$

9-6. Spin as a Classical Property

We know that if we consider the electron as the spinning sphere of charge, in such a case, given the small size of the electron ($r < 10^{-16}m$) [38] and based on the classical equation $L = I\omega$, ω will have a large value. A large w means a large peripheral velocity in the equator of the spinning sphere. Which in this case is higher than the velocity of light. But in our model, the electron is surrounded by a wave packet (Fig. 5). If we assume associated wave of a particle is dark matter, in such a case, due to the non-zero mass of dark matter, we can consider the spin of electron as a classical property. Dark matter has mass. Thus, associated wave packet of electron has a part of the mass of the electron, and in fact the mass that humans have measured for the electron, by different ways, is the mass of electron and its associated wave. The electron associated wave is much larger than the electron size ($r < 10^{-16}m$). As mentioned, for example, the wavelength of associated wave packet of an electron in the first orbit of a hydrogen atom is 3.3 angstroms. Thus, based on the equation $I = \int r^2 dm$ the moment of inertia of the electron (namely the moment of inertia of the particle along with its wave packet) increases and according to the equation $L = \sqrt{s(s+1)}\hbar = \frac{\sqrt{3}}{2}\hbar = I\omega$, ω decreases (which means that the wave packet of electron, like the electron, has a spinning motion). So based on our model, spin can be considered as a classic motion.

Particle experimenters have obtained the diameter of an electron by examining face-to-face collisions [38]. In these experiments, the diameter of the associated wave packet is not measured. The wave packet in collisions is transparent and low effect. The diameter of the wave packet usually is defined as one-half of maximum value of the function at the center.

Conclusion

In this article we proved that almost there is no doubt about the existence of a wave function in the solar system. Without the solar system wave packet, it is not possible to reach to the TBL from the protoplanetary disk. Can a theory other than wave theory explain the uniform and Isotropic distribution of mass in the asteroid belt? De Broglie considered the wave nature for subatomic particles, and here we attributed the wave nature to celestial objects. Neither of these two actions is strange. Rather, they are truths that we must become accustomed to.

It seems that the new atomic model is the final model of atom. This model is a unifying model that includes both the Schrodinger wave function and the Bohr atomic model inside. In fact, Niels Bohr and Schrodinger each were achieved to a piece of reality, and Figure 5 is probably total of reality and the final atomic model. We have noticed the existence of a wave along with an object since De Broglie. But we never thought it would be in the form of Figures 5 and 2.

In our opinion, prediction of the secondary lines of the hydrogen spectrum is a complete success for the new atomic model. Based on the new atomic model, normal Zeeman effect was more easily justified. Anomalous Zeeman effect, which is caused by the spin of electron, is also easily described by the new atomic model, which we have not described due to the length of the article.

Based on this article, the associated wave packet of an object (such as electron, proton or sun) is one of the candidates for the nature of dark matter.

Anyone familiar with the history of quantum mechanics and atomic models (especially the debates and problems of the third decade of the twentieth century such as Niels Bohr and Schrodinger debates about quantum jumps) will understand that what important problems have been solved in this article. Here, we proved that the word of " thought experiment " is meaningless and an experiment must be done in the real world so that we can talk about its results. In this article, we turned quantum mechanics into a simpler and more beautiful theory.

References:

[1]. Carrol, B. Ostlie, D. *An Introduction to Modern Astrophysics* (Cambridge University Press, Cambridge, ed. 2, 2017), pp. 716-717

[2]. Bohr, N. On the Constitution of Atoms and Molecules. *Philos. Mag.* ***26****, 1*, (1913)

[3]. Merton, T. Barratt, S. On the spectrum of hydrogen. Philosophical Transactions of the Royal Society of London. Series A, Containing Papers of a Mathematical or Physical Character 222: 369–400 (1922)

[4]. Allan, S. The band spectrum of hydrogen. Proc. R. Soc. Lond. **106**: 69–82, (1924)

[5]. Nicholson, J. The Secondary Spectrum of Hydrogen. *Nature* **105,** 166–167 (1920)

[6]. Richardson, O. The Secondary Hydrogen Spectrum. *Nature* **118,** 116 (1926)

[7]. Walker, J. Halliday, D. *Fundamentals of Physics.* (Wiley Ltd, ed. 10, 2007), pp. 449-450

[8]. Weidner, R. Sells, R. *Elementary Modern Physics* (Allyn and Bacon, ed. 2, 1973), pp 14-16

[9]. Michelson, A. Morley, E. On the Relative Motion of the Earth and the Luminiferous Ether. American Journal of Science. 34 (203): 333–345 (1887)

[10]. Branson, Jim. "Fourier Transform of Gaussian", *Quantum Physics* (April 2003). URL: https://quantummechanics.ucsd.edu/ph130a/130_notes/node88.html.

[11]. Gasiorowicz, S. *Quantum Physics* (John Wiley & Sons Inc, ed. 1, 1974), pp. 27-32

[12]. Cohen-tannoudji, C. Diu, B. *Quantum Mechanics.* (John Wiley & Sons Inc, Vol. 1, 1977), pp. 21-22

[13]. Ohanian, H. *Modern Physics.* (Prentice-Hall, Inc, 1987), pp. 198-200

[14]. Davisson, C. Germer, L. Diffraction of Electrons by a Crystal of Nickel. *Phys. Rev*. 30, 705. (1927).

[15]. Zeilik, M. *Astronomy. Ch. 14* (Cambridge University Press, ed. 9, 2002).

[16]. Bonanno, A. Schlattl, H. Paternò, L. The age of the Sun and the relativistic corrections in the EOS. *Astronomy and Astrophysics.* **390** (3). 1115–1118 (2002)

[17]. Williams, J. Cieza, L. Protoplanetary Disks and Their Evolution. *Annual Review of Astronomy and Astrophysics.* **49**: 67–117 (2011)

[18]. Rossing, T. The Physics of Kettledrums. *Scientific American,* **247**, No. 5, 172-179 (1982)

[19]. Bennett, J & et al. *The Essential Cosmic Perspective* (Addison-Wesley, ed. 6, 2012), page 165

[20]. Bennett, J & et al. *The Essential Cosmic Perspective* (Addison-Wesley, ed. 6, 2012), page 263

[21]. Eisberg, R. *Quantum Physics.* (John Wiley & Sons Inc, New York, ed. 2, 1974), pp. 134-135

[22]. Hoffmann, B. *The strange story of the Quantum.* (Dover Publications, 2011)
[23]. Zeilik, M. *Astronomy.* (Cambridge University Press, ed. 9, 2002)
[24]. Nieto, M. *The Titius-Bode Law of Planetary Distances: Its History and Theory.* (Pergamon Press, ed. 1, 1972).
[25]. Nieto, M. *The Titius-Bode Law of Planetary Distances: Its History and Theory.* (Pergamon Press, ed. 1, 1972) pp 62-63
[26]. Nieto, M. *The Titius-Bode Law of Planetary Distances: Its History and Theory.* (Pergamon Press, ed. 1, 1972) pp 71-75.
[27]. Nieto, M. *The Titius-Bode Law of Planetary Distances: Its History and Theory.* (Pergamon Press, ed. 1, 1972) pp 68-71.
[28]. Lynch, P. On the significance of the Titius–Bode law for the distribution of the planets, *Monthly Notices of the Royal Astronomical Society*, Volume 341, Issue 4, June 2003, Pages 1174–1178,
[29]. Arya, A. *Introduction to classical mechanics.* (Allyn & Bacon, ed. 1, 1990). pp. 248-251
[30]. Ritz, J. Milford, F. *Foundations of Electromagnetic Theory*. (Addison-Wesley, ed. 3, 1960). pp. 163-165
[31]. Weidner, R. Sells, R. *Elementary Modern Physics* (Allyn and Bacon, ed. 2, 1973), pp 240-247
[32]. Dieke, G. The molecular spectrum of hydrogen and its isotopes. *Journal of molecular spectroscopy* **2,** Issues 1–6. 494-517 (1958)
[33]. Richardson, O. *Molecular Hydrogen and its Spectrum.* (New Haven, Yale University Press; London, 1934).
[34]. Ohanian, H. *Modern Physics.* (Prentice-Hall, Inc, 1987) pp. 160-161
[35]. Eisberg, R. *Quantum Physics.* (John Wiley & Sons Inc, New York, ed. 2, 1974), page: 107
[36]. Eisberg, R. *Quantum Physics.* (John Wiley & Sons Inc, New York, ed. 2, 1974), pp 114-117
[37]. Mcevoy, J. Oscar, Z. Introducing Quantum Theory. (Icon Books, ed. 4, 2003)
[38]. Eisberg, R. *Quantum Physics.* (John Wiley & Sons Inc, New York, ed. 2, 1974), page: 277